Available online at www.sciencedirect.com

SCIENCE DIRECT®

Polymer 45 (2004) 3267–3276

polymer

www.elsevier.com/locate/polymer

Block-copolymer organic–inorganic networks. Structure, morphology and thermomechanical properties

Libor Matějka*, Oxana Dukh, Helena Kamišová, Drahomíra Hlavatá, Milena Špírková, Jiří Brus

Institute of Macromolecular Chemistry, Academy of Sciences of the Czech Republic, Heyrovskú Sq. 2, 162 06 Prague 6, Czech Republic

Received 4 November 2003; received in revised form 27 February 2004; accepted 5 March 2004

Abstract

Structure, morphology and thermomechanical behaviour of organic–inorganic (O–I) networks prepared from O–I precursors were studied. The networks from two types of the precursors were formed (a) by the hydrolytic polycondensation of the alkoxysilane-endcapped oligomers (ASO) and (b) from epoxy-functional silsesquioxane (SSQO) clusters (EC) by reaction with an oligomeric diamine, JEFFAMINE D2000. The O–I block copolymer networks are composed of regularly arranged SSQO domains forming junctions of the network linked by oligomer chains. Structure of the SSQO 'crosslinks' ranges from compact polyhedral cages of size 1–3 nm in the networks from ASO to 5–15 nm spherical SSQO clusters in the stoichiometric networks EC-D2000. Large interconnected SSQO cylinders 30–150 nm in diameter arranged in a continuous ladder-like structure are formed at deficiency of the amine. Bicontinuous morphology results in a significant reinforcement. Interphase H-bond interaction between SiOH of SSQO domains and the organic chain leads to the chain immobilization and affects glass transition temperature and mechanical properties.

© 2004 Published by Elsevier Ltd.

Keywords: Organic–inorganic hybrid; Polymer network; Sol–gel process

---

1. Introduction

Organic–inorganic (O–I) hybrid networks formed by the so called sol–gel process are microphase-separated systems showing various structures and morphologies. These hybrids consist either of O–I interpenetrating networks with bicontinuous phases or both organic and inorganic network may serve as a matrix hosting dispersed domains of the other phase. Due to the small size of the molecularly dispersed heterogeneity domains in the nanoscale region, the hybrids are regarded as O–I nanocomposites and show a very large interface area. Therefore, interphase interactions are crucial for final morphology and especially for material mechanical properties. In order to strengthen this interaction coupling agents are often used to form interphase covalent bonding. O–I precursors containing both organic and inorganic functionalities capable of forming the corresponding structures are convenient reagents. The inorganic structures are formed by the sol–gel process involving hydrolysis and condensation of, e.g. alkoxysilane groups. The polymerization of organic and inorganic functionalities results in the formation of the O–I block copolymer hybrid networks. The morphology model of the O–I networks assumes organic- and inorganic-rich phases as well as a mixed interphase [1]. Structure and morphology of the O–I networks determining their material properties can be tailored by reaction conditions in synthesis or by using precursors of crosslinking of various molecular architecture. Investigation of crosslinking of the O–I precursors makes it possible to get general knowledge on how to control the network build-up and the final nanocomposite structure, morphology, interphase interaction and properties.

We have studied the O–I block copolymer networks synthesized from two different types of the O–I precursors—alkoxysilane-endcapped oligomers (ASO) and silsesquioxane (SSQO) clusters containing epoxy functionalities (EC). The ASO were crosslinked by the hydrolytic condensation of the functional groups at the chain extremities to produce SSQO junction domains of the forming O–I hybrid network. In the second system, first the well defined SSQO domains, EC, were prepared and then interlinked by the reaction with oligomeric diamines, JEFFAMINE, to build the O–I network. Structure evolution

---

* Corresponding author. Tel.: +420-296809281; fax: +420-296809410.
E-mail address: matejka@imc.cas.cz (L. Matějka).

0032-3861/$ - see front matter © 2004 Published by Elsevier Ltd.
doi:10.1016/j.polymer.2004.03.033

and network formation during crosslinking polymerization of precursors of various architecture as well as microphase separation in these systems are described in a previous paper [2]. For a better understanding, the structure was also studied using model systems. Organotrialkoxysilanes with a long-chain organic substituent, i.e. oligomers capped with alkoxysilane groups at one end only, were used as models for crosslinking of ASO. These low-functional reagents do not gel due to their high tendency to cyclization [3] and the soluble products are easy to analyze. Long substituents were found to impose a severe steric restriction to intermolecular sol–gel condensation of alkoxysilane groups and hence a preferred intramolecular condensation occurs in particular under basic or dibutyltin dilaurate (DBTDL) catalysis. This leads to the formation of compact polyhedral SSQO oligomers mainly octamer ‘cage’ structures with pendant organic substituent chains. Accordingly, the gelation mechanism proposed for oligomers silane-capped at both ends (ASO) assumes formation of cages at an early reaction stage serving as building units in crosslinking. In contrast, acid-catalyzed systems undergo production of loose branched SSQO structures. In the reaction of epoxy-functional SSQO clusters (EC) with poly(oxypropylene)-diamine, first the cluster growth occurs by intermolecular sol–gel condensation initiated with basic amine followed by the epoxy-amine crosslinking addition reaction.

In this paper, the morphology, interphase interaction and thermomechanical properties of both types of the O–I networks were determined using ^{29}Si NMR, small-angle X-ray scattering (SAXS), atomic force microscopy (AFM), dynamic mechanical analysis (DMA) and tensile stress–strain mechanical measurements. Polybutadiene and polycaprolactone chains containing O–I networks were followed, however, most of the studied networks were based on the poly(oxypropylene). The networks from the alkoxysilane-endcapped poly(oxypropylene) were recently investigated by Jordens and Wilkes [4] as a novel ceramer material. Our new approach in the O–I network study consists in the comparison of two types of the networks formed by different procedures and different reaction mechanisms from ASO and silsesquioxane EC. The SSQO clusters form crosslink domains of the O–I network linked with the same oligomer chains in both cases. However, different synthesis approach and molecular architecture of the precursor result in different structure, morphology and properties. We have analyzed the structure of the O–I block copolymer based network including the inner structure of the SSQO junction domains. It is known [5,6] that the distance between inorganic cluster domains correlates with the length of the polymer chain. The inner structure of the inorganic domains, however, is less understood. In this paper, moreover, the effect of the gelation mechanism and network formation on the morphology, network structure and mechanical properties is discussed. Also the results obtained from model systems are used to assist the interpretation of the network structure. The O–I polymers, showing excellent properties described in literature [7], were usually prepared by polymerization in the presence of tetraethoxysilane (TEOS) or tetramethoxysilane (TMOS) in order to increase the inorganic phase fraction in the hybrid. We have also studied the effect of TEOS in the network, however, the stress is put mainly on structure analysis and an increase in the inorganic phase would be necessary to improve mechanical properties of the material.

2. Experimental

2.1. Synthesis and description of O–I networks and models

Synthesis of the O–I networks from (a) ASO or (b) epoxy-functional SSQO clusters (EC) was described in a previous paper [2]. The networks and models designation and characterization are given in Table 1.

(a) Poly(oxypropylene) (POP), polybutadiene (PB) and poly(ε-caprolactone)(PCL) of various molecular weights were endcapped with alkoxysilane groups and crosslinked in the presence of water by sol–gel polymerization. The ASO were prepared by modification of oligomeric diols or diamines with (3-isocyanatopropyl)-triethoxysilane (ITES). The linkage character of the alkoxysilane to an oligomer was shown to catalytically affect the crosslinking sol–gel process [2,3]. Modification of diols and diamines with ITES results in urethane or urea linkage, respectively, (see Table 1). The urea grouping in JEFFAMINE-based precursors effectively catalyzes the sol–gel condensation and influences the final network structure. A stoichiometric amount of water was used in the sol–gel crosslinking polymerization corresponding to the ratio $r_{HS}(=[H_2O]/[Si])=1.5$. *p*-Toluenesulfonic acid (TSA), DBTDL or benzyldimethylamine (BDMA) were applied as catalysts for the sol–gel reaction. The hybrids with high inorganic fraction were prepared by copolycondensation of ASO with TEOS.

Table 1
Description of the O–I networks and model systems

	Organic backbone, *M*	Coupling agent, linkage group
ASO-based networks		
SPPGx[a]	POP, 1200, 2000	ITES, urethane
SDx	POP, 400, 2000, 4000	ITES, urea
SPBx	PB, 2000	ITES, urethane
SPCLx	PCL, 2000	ITES, urethane
SPPGx-TEOS	POP, 2000	ITES, urethane
EC-based networks		
EC-Dx	POP, 400, 2000	–, amine
Model systems		
SPEOx	POE, 750	ITES, urethane
EC-Mx	POP, 600, 2650	–, amine

[a] x—Molecular weight of the oligomer.

(b) The SSQO clusters with epoxy functionalities were prepared by sol–gel polymerization of GTMS [8]. These clusters were then crosslinked with oligomeric diamines D2000 or D400. The composition of the networks was characterized by the ratio of the epoxy and amine functionalities $r_{\mathrm{AE}}(= [\mathrm{NH}]/[\mathrm{epoxy}])$.

(c) The O–I models—oligomers silane-capped at one end only, e.g. α-hydro-methoxy poly(oxyethylene) modified with the trialkoxysilyl group, and EC-monoamine (JEFFAMINE M600 and M2005) systems were used for structure analysis.

The investigated networks differ in synthetic procedure, chemical character and the length of the organic backbone. The bonding to the formed SSQO structure and the inorganic phase content also differ (see Table 1). The network designation is as follows, e.g.: SPPG2000/TSA indicates the network prepared from silane-modified poly(propylene) glycol of molecular weight $M \sim 2000$ using TSA as a catalyst for sol–gel polymerization; SD2000 denotes a network formed from silane-modified D2000; EC/TSA-D2000 means the network from epoxy-functional clusters prepared under TSA catalysis and crosslinked with D2000.

The network samples were prepared at 80 °C in Teflon molds, postcured for 24 h at 120 °C and vacuum dried before analysis. All samples were transparent; their extraction was performed with acetone and toluene.

2.2. Methods

^{29}Si and ^{13}C NMR spectra were measured with a Bruker DSX 200 NMR spectrometer. The conversion α_{Si} of formation of siloxane bonds in the sol-gel process was determined as $\alpha_{\mathrm{Si}} = (\sum iT_i)/3$, where T_i indicates fraction of the unit T_i with i siloxane bonds Si–O–Si– attached to the central silicon. ^{13}C NMR analysis was used to determine conversion of the epoxy groups [8].

SAXS measurements were performed using an upgraded Kratky camera with a 60 μm entrance slit, 42 cm flight path and Ni-filtered Cu K_α radiation (wavelength $\lambda = 1.54$ Å). The measured intensities were corrected for sample thickness and transmission, primary beam flux, and sample-detector distance. However, no corrections for the primary beam profile were used.

Atomic force microscopy (AFM) measurements were performed under ambient conditions using a commercial atomic force microscope (MultiMode Digital Instruments NanoScope™ Dimension III). Olympus oxide-sharpened silicon nitride probes (OMCL TR-400) in the contact mode was used. The normal force of the tip on the sample was reduced and did not exceed values of 10 nN in order not to damage the samples. Sample surfaces fractured in liquid nitrogen were scanned.

Rheometer ARES (Rheometric Scientific) was used to follow the dynamic mechanical behaviour of the networks. The temperature dependence of the complex shear modulus of rectangular samples was measured by oscillatory shear deformation at a frequency of 1 Hz.

Static mechanical properties were measured on an Instron model 6025 (Instron Limited). Samples of the size 30 × 9 × 1 mm were tested at laboratory temperature and a test speed of 3.33×10^{-2} mm/s.

3. Results and discussion

3.1. Morphology of the O–I networks

The O–I networks are heterogeneous systems and SAXS and AFM provide an evidence of the microphase separation of organic and SSQO phases. In the O–I model systems—organotrialkoxysilanes and EC-monoamine in solution—it was proved that the structure composed of SSQO domains with emanating organic chains is well ordered [2,3]. The structure of the O–I networks is also well ordered, as one can see from SAXS profiles in Fig. 1. The figure shows the effect of the synthetic procedure and molecular architecture of the precursor (Fig. 1(a)) including the oligomer length (Fig. 1(b)), catalytic reaction conditions (Fig. 1(c)) or presence of TEOS (Fig. 1(d)) on the final morphology. The interference maxima in the figures indicate a two-phase structure and a regular arrangement of the SSQO clusters forming junctions of the block copolymer O–I networks. Position of the maximum of the scattering vector $q_{\max}$ is given by the interjunction spacing $d(= 2\pi/q_{\max})$, correlating with the length of the corresponding linking oligomer chain in agreement with literature data [1,5]. Fig. 1(b) shows the shift of the maximum with the oligomer length of the networks prepared from oligomers of various molecular weights, $M = 400$, 2000 and 4000.

The majority of the networks synthesized by using oligomers of molecular weight $M \sim 2000$; both from alkoxysilane-modified oligomers (ASO) and functional SSQO clusters (EC), show SAXS intensity interference maxima in the region $q_{\max} = 0.135 - 0.15 \text{Å} - 1$ (see Fig. 1(a)). These maxima correspond to the correlation distance 42–46.5 Å in accordance with the results of Jordens and Wilkes [4] who found a spacing of 45 Å in the networks from silane-endcapped D2000. However, in SPPG2000 networks we have observed a shift of the maximum to a higher q-value ($q_{\max} = 0.175 \text{Å}^{-1}$) in the systems polymerized using an acid catalyst (TSA) compared to those catalyzed with a base (BDMA) as can be observed in Fig. 1(c)—curves 1 and 2. The acid catalysis of the sol–gel process promotes hydrolysis [9] leading to a high content of –SiOH in the SSQO clusters and a strong H-bond interaction with $-\mathrm{OCH_2}-$ groups in POP chains. Due to this interaction in contrast to basic catalysis a partial mixing of the organic chains and SSQO domains occurs, which improves compatibility, decreases the correlation distance and shifts the interference maximum to a higher q-value.

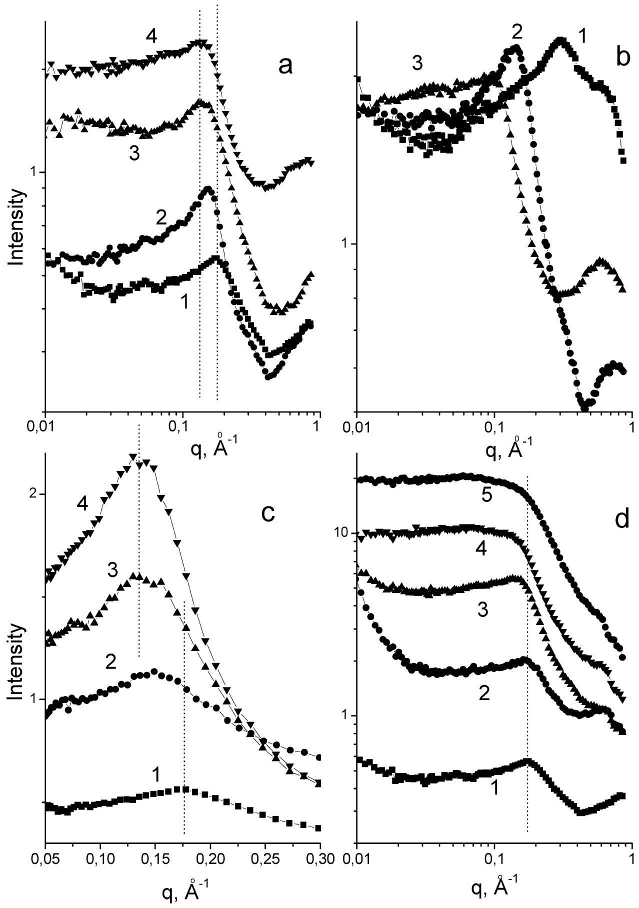

Fig. 1. SAXS profiles of the O–I networks prepared (a) from various precursors; 1-SPPG2000/TSA, 2-SD2000, 3-SPB2000/TSA, 4-EC/TSA-D2000; (b) from oligomers of various molecular weight 1-SD400, 2-SD2000, 3-SD4000; (c) under acid (TSA) and basic (BDMA) catalysis 1-SPPG2000/TSA, 2-SPPG2000/BDMA, 3-SPB2000/TSA, 4-SPB2000/BDMA; (d) with variable contents of TEOS SPPG/TSA-TEOS, wt % TEOS 1–0%, 2–9.1 wt%, 3–28.6 wt%, 4–47.4 wt%, 5–64.3 wt%.

Contrary to this, an internal basic catalysis with urea grouping in SD2000 (cf. Table 1) is a reason for a worse compatibility and a larger interdomain distance compared to SPPG2000/TSA network in Fig. 1(a). Low compatibility is characterized by a sharp interference peak and a steep slope of SAXS intensity profiles in the Porod region at high q. This is also in accordance with the fact that loose SSQO structures formed under acid catalysis are more capable of interface interaction than the compact structures produced using basic catalysts. On the other hand, no such shift of the maximum due to catalysis occurs in the networks prepared from alkoxysilane-endcapped polybutadiene, SPB2000 (cf. Fig. 1(c), curves 3 and 4). In this case there is no interaction with polybutadiene chains. Therefore, the SPB based networks are strongly microphase separated as indicated by a steep slope of the SAXS curve. The networks formed by crosslinking of EC with D2000 show less pronounced maxima (cf. Fig. 1(a) curve 4) revealing that the SSQO domains arrangement is less regular. Moreover, $q_{\max}$ is slightly shifted to a lower value corresponding to a longer correlation distance and to larger clusters compared to the network from SPPG2000 and SD2000. The increasing size of the cluster namely results in a larger correlation distance [6].

The discussed O–I networks from O–I precursors contain only a low proportion (5 wt%) of inorganic structures. The systems with a higher content of an inorganic phase were synthesized by copolycondensation of ASO with TEOS. Fig. 1(d) shows the SAXS profiles of the networks from SPPG2000 with various contents of TEOS. With increasing TEOS amount, the scattered intensity increases, $q_{\max}$ shifts to a lower value, the peak broadens and, at sufficiently high TEOS concentration (~ 60 wt%), the maximum disappears. Sol–gel polymerization of TEOS results in the formation of silica domains dispersed in a matrix. In addition, cocondensation with the alkoxysilane groups of SPPG2000 takes place enlarging junction 'points', which leads to a shift of the maximum. In contrast to the neat SPPG2000 network, inorganic clusters in SPPG2000–TEOS are formed not only at the organic chain ends but also irregularly along the chain. Disappearance of the interference maximum is the result of such an irregular arrangement and increasing connectivity between silica domains possibly forming the continuous phase. A continuous silica phase was observed by Rodrigues et al. [6] using electron microscopy in the network based on poly(tetramethylene oxide) and TEOS at a high TEOS content.

The O–I hybrid morphology observed by AFM is shown in Fig. 2. In the case of EC-D2000 networks with stoichiometric composition, $r_{AE} = 1$ (Fig. 2(a)), the spherical objects of 5–15 nm in diameter are spread on the fractured surface. These spherical domains correspond to the SSQO clusters interlinked by D2000 chains. The networks prepared with deficiency of an amine, show a different structure. The morphology of the EC-D2000 networks with $r_{AE} = 0.2$ is given in Fig. 2(b) and (c). The structure consists of SSQO cylinders, 30–150 nm in diameter. Detail in Fig. 2(c) reveals that the cylinders are interconnected. As to the ASO-based networks, we have not obtained convincing results using AFM. The fractured surface of the SD2000/DBTDL network is quite rough and we failed to get a sufficiently good resolution. Nevertheless, the data do not reveal any structure features corresponding to objects larger than 3 nm. Consequently, the small SSQO clusters of size 1–2 nm proved in model systems [2] are likely present as the network junctions. This agrees with the results of Cuney et al. [10] who found the particles of diameter 1.5 nm at the chain ends in the network of silane-endcapped hydrogenated PB.

3.2. SSQO 'crosslink' domain

^{29}Si NMR results show that conversion of Si-units α_{Si} in the SSQO domains of the O–I networks formed both from ASO and EC depends mainly on catalysis of the sol–gel

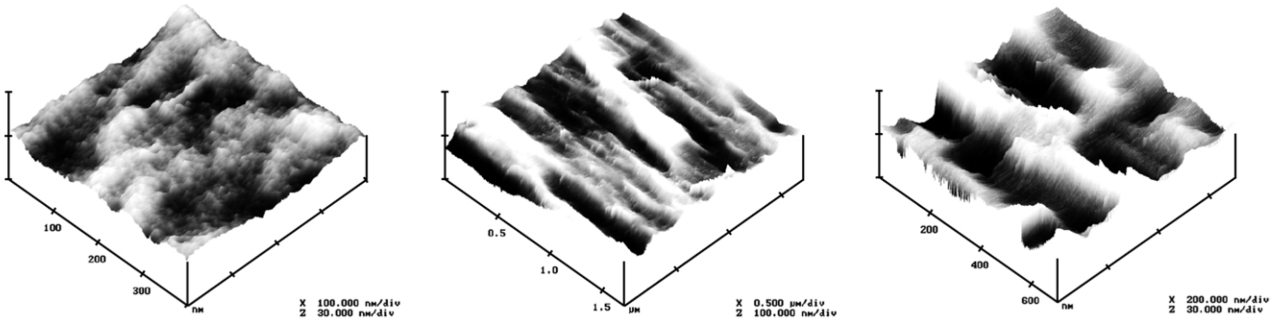

(a) (b) (c)

Fig. 2. AFM scans of EC/TSA-D2000 networks: (a) $r_{AE} = 1$; (b) $r_{AE} = 0.2$; (c) $r_{AE} = 0.2$ —detail.

reaction. Acid catalysis, using TSA, results in a relatively low overall conversion, $\alpha_{Si} = 0.85 - 0.91$ (see Table 2) and a high content of unreacted SiOH. On the contrary, a higher conversion was achieved using neutral DBTDL and basic BDMA catalysts, which promote condensation [9]. The effect of catalysis on the final curing is obvious also from a higher conversion in the networks based on SD compared with those based on SPPG. Internal catalysis with the urea grouping present in the SD precursor enhances condensation [2,3] and leads to a high conversion (Table 2). Under given catalytic conditions, the final α_{Si} conversion is the same both in the network from ASO and in the soluble SSQO polymerization product of a model organotrialkoxysilane. Distribution of the Si units both in the cured network SPPG2000/DBTDL and the model SPEO750/DBTDL is: $T_2 = 0.28$, $T_3 = 0.72$, respectively. This implies that formation of the SSQO structure as a branching domain in the O–I network is not restricted with respect to polymerization of the models and justifies application of the models to network characterization.

The AFM data and results from models support gelation mechanism proposed in Ref. [2] and provide indirect evidence of the SSQO domain structure in cured networks. The junctions of the network from endcapped oligomers crosslinked under DBTDL or basic catalysis consist of the small, highly condensed, compact cage-like SSQO structures. On the contrary, the 'crosslinks' in the networks built under acid catalysis are assumed to be composed of less condensed, loose SSQO clusters with a high content of unreacted SiOH. In the case of the EC-based networks the SSQO domains are larger or even form a continuous cylinder-like phase involving compact polyhedral structures.

Table 2
Conversion α_{Si} in SSQO domains of the O–I networks and in the initial EC

System		Conversion	
Network	Catalysis[a]	Network	EC[b]
EC-D2000	TSA	0.85–0.89	0.3–0.65
	DBTDL	0.91–0.95	0.65–0.85
	BDMA	0.97	0.95
SPPG2000	TSA	0.86–0.91	
	DBTDL	0.91	
SD2000	TSA	0.95	
	DBTDL	0.97	

[a] In sol–gel crosslinking of ASO or synthesis of the EC.

[b] In the precursor EC, the conversion is controlled by the reaction time in the EC synthesis.

3.3. Network structure

The basic characteristics of a network structure are given by crosslinking density ν defined as the concentration of elastically active network chains. In an ideal case of a homogeneous network without defects and dangling chains, ν is determined by the molecular weight M_c of the chain between junctions, $\nu \sim 1/M_c$, assuming only covalent crosslinks are formed. According to the Flory–Erman (F–E) rubber elasticity theory [11], the crosslinking density is related to the equilibrium shear modulus G_e in the rubbery state; $G_e = \nu ART$. (Front factor $A = (f_{eff} - 2)/f_{eff}$ for a phantom network with no interaction between network chains and free fluctuation of junctions and $A = 1$ for the affine network where the crosslinks do not fluctuate and are displaced affinely with a macroscopic strain. f_{eff} is the effective functionality of the crosslink). Contrary to classic networks with point-like crosslinks, in the studied O–I networks the junction is formed by a 'crosslink domain'. Such networks can be treated by considering SSQO junctions as inelastic hard clusters of various sizes and 'crosslink functionality'. Within hard clusters the chains between branch points are too short and, therefore, elastically inactive. However, according to the concept of hard clusters in heterogeneous networks [12], the loss of elastically active network chains in the cluster is fully compensated by a higher cluster functionality. Hence, the crosslinking density can be calculated by the classic theory. In heterogeneous systems, however, mechanical properties and the modulus depend on a system morphology, e.g. phase continuity or discontinuity, volume fraction of different phases and interface interaction. The SSQO and silica domains in the O–I hybrids serve as a hard filler dispersed in an organic matrix and under particular conditions a bicontinuous O–I morphology is formed. Mechanical behaviour and rubbery modulus in the former case, i.e. the particulate composite, are described by Kerner–Nielsen model [13], $G_C = G_M(1 + 1.5V_f)/(1 - \Psi V_f)$, assuming that $G_f \gg G_M$ and Poisson ratio of the matrix in the rubbery state is equal to 0.5, $\Psi = 1 + V_f(1 - V_{max})/V_{max}^2$. G_C, G_M and G_f are moduli of the composite, matrix and the inorganic filler phase, respectively; V_f and V_{max}, are volume fraction and the maximum packing fraction of the filler. The heterogeneous systems with bicontinuous morpohology are often treated by using empirical Davies model [14]: $G_C^{1/5} = V_M G_M^{1/5} + V_f G_f^{1/5}$ where V_M is volume fraction of the organic matrix.

Table 3 shows dynamic shear storage moduli G' of the studied O–I networks in the rubbery state. Due to a relatively high crosslinking density of the networks, modulus relaxation is fast. Therefore, the moduli measured at temperatures at least 50 °C above T_g, at a frequency of 1 Hz, are close to the equilibrium values. Included are also theoretical values calculated (a) from concentration of elastically active chain (EAC)s using F–E theory, (b) taking into account the inorganic filler effect by using Kerner–Nielsen model and (c) assuming a bicontinuous morphology according to the Davies model. The experimental moduli of ASO-based networks in Table 3 are in good agreement with theory taking into account both the crosslinking density determined by concentration of the elastic oligomer and the filler effect. The decreasing size of the oligomer corresponds to an increase in crosslinking density and hence the networks prepared from shorter precursors PPG1200 or D400 show higher moduli. An efficient reinforcement, however, was achieved mainly in the systems with a high TEOS content where the continuous silica phase appears [15]. Also off-stoichiometric EC-D2000 network ($r_{AE} = 0.05$) with the continuous inorganic phase (cf. Fig. 2(c)) exhibits a high modulus. The systems with a bicontinuous morphology are satisfactorily described by Davies model, assuming that fraction c of the inorganic structure forms the continuous phase.

Table 3
Rubbery shear modulus of the stoichiometric O–I networks

Network	G', 10^6 Pa (at 25 °C)			
	Experimental	Calculated		
		F–E	Kerner	Davies
SPPG2000	1.6	1.3	1.5	
SD2000	1.6	1.25	1.4	
SPB2000	1.7	1.25	1.4	
EC-D2000	3.6	3.2[a]	3.6[a]	
SPPG1200	3.5	1.9	2.2	
SD400	4.1[b]	4.4	5.7	
EC-D400	9.9	8.5[a]	12.3[a]	
SPPG2000-TEOS (47 wt%)	8.7[b]	1.5	2.2	9 ($c = 0.75$)
SPPG2000-TEOS (64 wt%)	44[b]	1.5	2.8	36 ($c = 1$)
EC-D2000, $r_{AE} = 0.05$[c]	9.5			12 ($c = 0.5$)

F–E theory: $A = 1$; conversions given in Table 2 are taken into account. Kerner model: $V_{max} = 0.6$. Davies model: c, fraction of the inorganic structure forming the continuous phase. $G_f = 4 \times 10^9$ Pa for SiO_2, $G_f = 2 \times 10^9$ Pa for SSQO.

[a] Assumption that 3 elastically active chains are contributed by an oligomer.

[b] Measured at $T = 100$ °C.

[c] Off-stoichiometric network.

The data reveals that the EC-D2000 network has a significantly higher modulus compared to those formed from the ASO of similar molecular weights. The fraction of the hard inorganic structures is 4.9 and 7.8 wt%, respectively, in the SPPG2000 and EC-D2000 networks. The analysis based on the Kerner model shows that with such a small difference, the 'filler' effect cannot account for the higher modulus of the EC-D2000 network compared to the SPPG2000 network. Therefore, we assume that the reason for the increased modulus is a higher system functionality. In the case of the SPPG2000 or SD2000 networks, the precursors prepared by modification with ITES are bis-trialkoxysilane (polyoxypropylene)s. On the contrary, diamine D2000 reacts as a tetrafunctional agent, with the epoxy groups of EC, to form the EC-D2000 network. As a result, in the SPPG2000 network the precursor presents one elastically active chain (EAC) connecting the SSQO junctions, whereas in the EC-D2000 there are two trifunctional branch points at the ends of the D2000 chain. Therefore, in addition to one elastically active long chain there are four short chain sequences issuing from the branch points to the SSQO cluster. These flexible short sequences may contribute to the retractive force at deformation to some extent and increase the concentration of EAC. Analysis shows that the contribution of the each short sequence by 1/2 of the EAC, i.e. three EAC per oligomer, leads to an approximate agreement with the experiment (see Table 3).

The EC-D2000 network shows features of typical epoxy-amine networks where mainly the composition (r_{AE}) of a system affects structure and properties. The ideal epoxy-amine network exhibiting the highest crosslinking density and no sol fraction is formed under stoichiometric conditions of functional groups ($r_{AE} = 1$). This is the case of a low-temperature curing process when only the epoxy-amine addition reaction takes place. Under a high temperature curing or base-catalysis the homopolymerization of epoxy groups occurs and crosslinking density increases at epoxy excess [16,17]. Effect of the composition (r_{AE}) on the network structure in the case of the hybrid EC/TSA-D2000 is shown in Fig. 3. For the low-temperature curing at 80 °C (curve 1), the maxima of the gel fraction (Fig. 3(a)) and of the modulus (Fig. 3(b)) are achieved at the stoichiometric composition. At an amine excess ($r_{AE} > 1$) both the gel fraction and modulus decrease and at the critical molar ratio, $(r_{AE})_c = 7.1$, no gel is formed. At an epoxy excess ($r_{AE} < 1$), the modulus and fraction of the gel decrease much less with increasing off-stoichiometry. Postcuring at a high temperature ($T = 120$ °C) (curve 2) results in a subsequent increase in modulus and the gel fraction of the

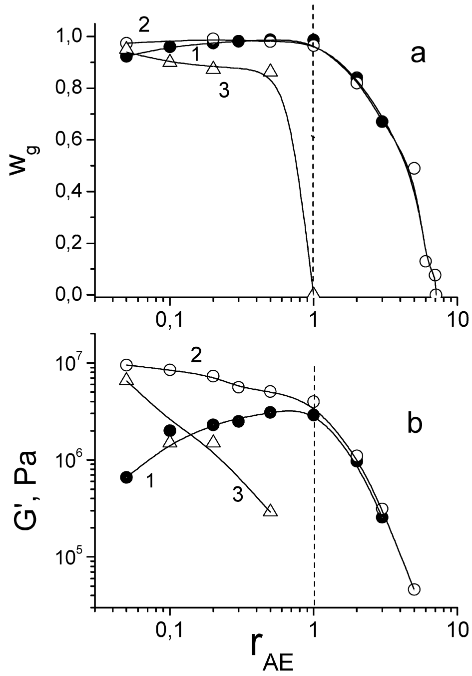

Fig. 3. Gel fraction w_g (a) and rubbery shear modulus G' (b) of EC/TSA-amine networks. 1 EC/TSA-D2000, $t_{cure} = 24$ h, $T = 80$ °C, 2 EC/TSA-D2000, $t_{cure} = 24$ h, $T = 120$ °C, 3 EC/TSA-M2005, $T = 120$ °C.

networks with epoxy excess and, finally, these systems achieve a higher modulus and w_g compared to the stoichiometric network. On the contrary, the right-hand side of the plot, i.e. that corresponding to the networks with an amine excess, does not change with the postcuring. Obviously, at an amine deficiency another crosslinking process takes place at the high temperature in addition to the epoxy-amine reaction. Homopolymerization of the excessive epoxy groups or formation of the SSQO network should be taken into account. ^{29}Si and ^{13}C NMR analysis show an increase in condensation conversion, α_{Si}, during high temperature curing while no change in the epoxy conversion was detected thus excluding epoxy homopolymerization. Consequently, a significant increase in modulus at high temperature curing is brought about by growth of the SSQO structure. The evidence of the SSQO development leading to the formation of the network with continuous SSQO structure was obtained also by using the model EC-monoamine M2005 cured at 120 °C. Due to steric reasons, both hydrogens of the NH_2 group in the monoamine react intramolecularly with epoxy groups of the same EC. Therefore, no network is formed, $w_g = 0$, by the epoxy-amine reaction under stoichiometric conditions or at amine excess ($r_{AE} > 1$) (Fig. 3(a), curve 3). Only at a deficiency of the amine the system gels, due to SSQO structure percolation. Hence, both the gel fraction and modulus increase with decreasing amine content as shown in Fig. 3.

Fig. 4 shows the effect of composition of the EC-D2000 networks on SAXS profiles. The stoichiometric network EC-D2000 (curve 1) exhibits the interference maximum at $q = 0.135\text{Å}^{-1}$ corresponding to the correlation distance given by the length of D2000 chain. At the amine deficiency $r_{AE} = 0.2$ (curve 2), this maximum becomes less pronounced and it disappears completely at $r_{AE} = 0.05$ (curve 3). New interference maximum appearing in these networks at $q = 0.42 - 0.45\text{Å}^{-1}$ is assigned to the correlation distance due to the unreacted (glycidyloxy)propyl groups separating the clusters. The result is in accord with the structure assumed in model systems in Ref. [2] (Scheme 3(d) in Ref. [2]).

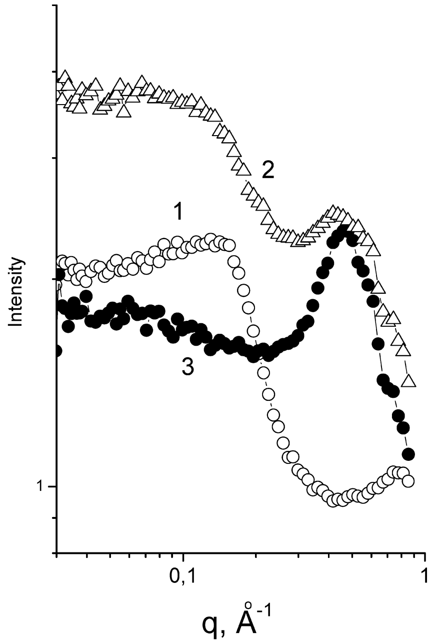

Fig. 4. The effect of composition r_{AE} on SAXS profiles of EC/TSA-D2000 networks. (1) $r_{AE} = 1$, (2) $r_{AE} = 0.2$, (3) $r_{AE} = 0.05$.

Concluding, DMA and SAXS analysis as well as AFM data are in perfect agreement with structure of model systems and gelation mechanism described in ref. [2] (Scheme 3 in Ref. [2]). They reveal both the structure of EC-diamine network and the crucial effect of the composition. The EC-D2000 structure is shown in Scheme 1. Stoichiometric O–I networks or those with amine excess involve relatively small, regularly arranged SSQO cluster junctions interlinked by the organic chains of D2000 (cf. Fig. 2(a) and Fig. 4—curve 1). The crosslinking density and fraction of the gel increase when approaching the stoichiometric composition, as in typical epoxy-amine networks (cf. Fig. 3). The system with deficient amine (Scheme 1(b)), however, is dominated by the large cylindric SSQO domains

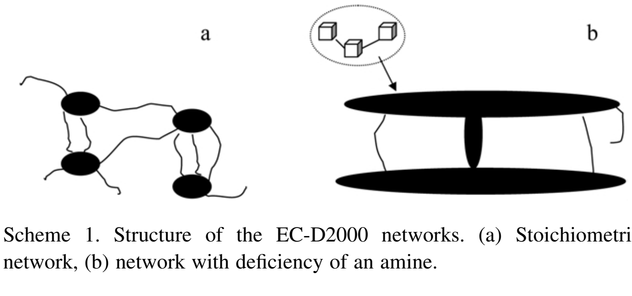

Scheme 1. Structure of the EC-D2000 networks. (a) Stoichiometric network, (b) network with deficiency of an amine.

separated by organic chains of the oligomeric amine (cf, Fig. 2(b)). Study of model systems showed [2] that large SSQO clusters are composed of condensed cage-like structures. The cylinders become interconnected reaching finally a percolation threshold to form the SSQO network (cf. Fig. 2(c)). The presence of the continuous SSQO structure accounts for the high gel fraction and modulus of highly off-stoichiometric networks at $r_{\mathrm{AE}} < 1$ (cf. Fig. 3).

3.4. Interphase interaction and thermomechanical properties

The thermomechanical behaviour of the O–I networks is characterized by temperature dependence of the shear modulus and the loss factor tan δ in Figs. 5–7.

The glass transition temperature T_g of the networks is determined first of all by the chemical nature of an oligomer chain as shown in Fig. 5 describing the networks with PB, PCL and POP backbones with $M \sim 2000$. SPB2000 network exhibits the highest $T_g(= -27\ ^\circ\mathrm{C})$ and the poly(oxypropylene)-based network SD2000 has $T_g = -55\ ^\circ\mathrm{C}$. The SPCL-based network shows a more complex behaviour because of crystallization. In addition to glass transition at $-60\ ^\circ\mathrm{C}$, melting of the backbone occurs at $T_m \sim 40\ ^\circ\mathrm{C}$. The glass transition temperature was taken as a temperature of the maximum of the loss factor tan δ corresponding to relaxation of organic chains at a measurement frequency of

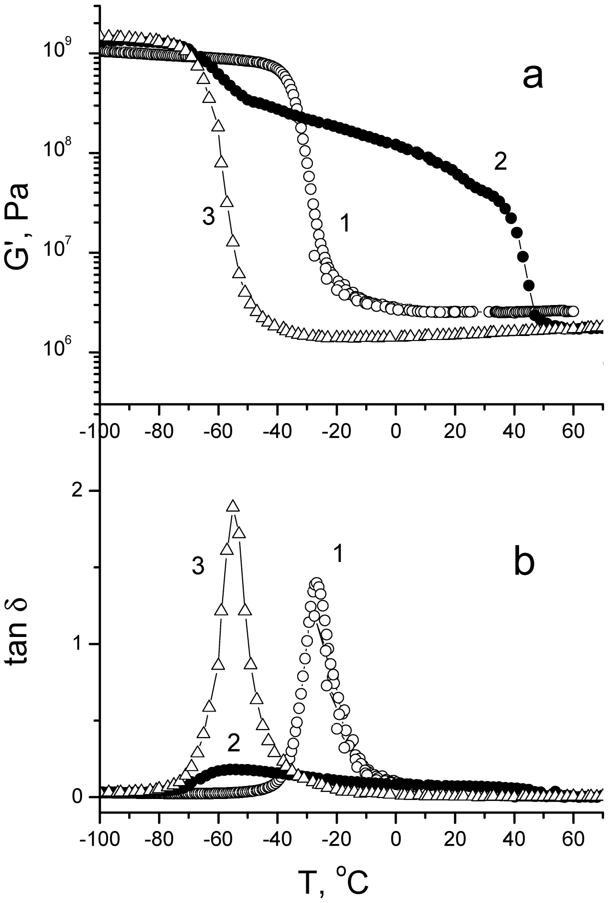

Fig. 5. Shear storage modulus G' (a) and loss factor tan δ (b) of O–I networks as a function of temperature. 1 SPB2000, 2 SPCL2000, 3 SD2000 (POP backbone).

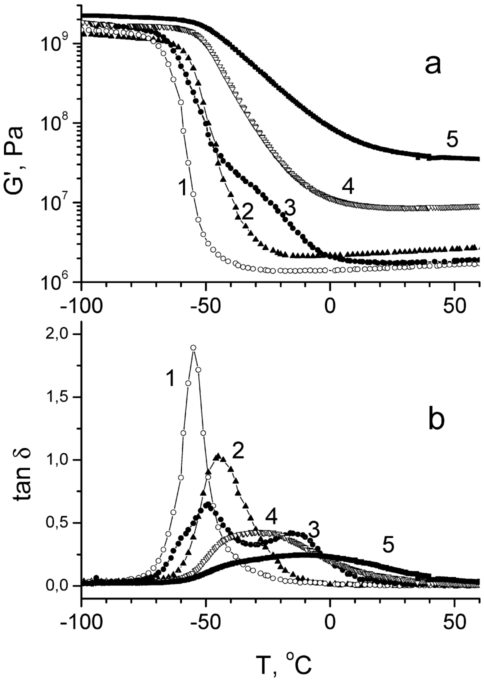

Fig. 6. Shear storage modulus G' (a) and loss factor tan δ (b) of poly(oxypropylene)-based O–I networks as a function of temperature. 1 SD2000, 2 EC/TSA-D2000, 3 SPPG2000/TSA, 4 SPPG2000/TSA-TEOS(47 wt % TEOS), SPPG2000/TSA-TEOS(64 wt% TEOS).

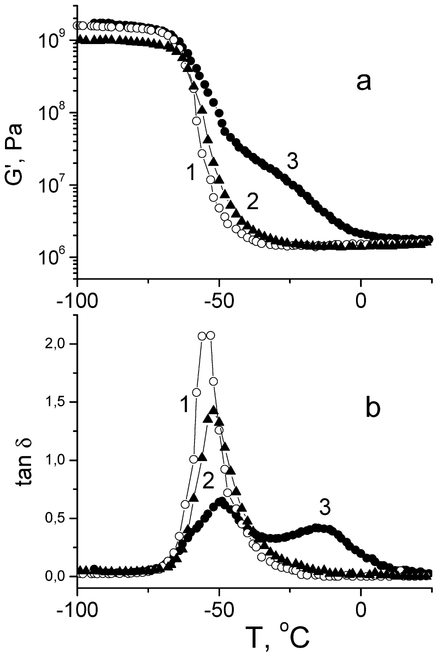

Fig. 7. Shear storage modulus G' (a) and loss factor tan δ (b) of SPPG2000 networks differing in conditions for hydrolysis of the sol-gel process. 1 SPPG2000/BDMA, 2 SPPG2000/TSA, $r_{\mathrm{HS}} = 0.5$, 3 SPPG2000/TSA, $r_{\mathrm{HS}} = 3$.

1 Hz. Figs. 6 and 7 show the effect of the O–I precursor type and interphase interaction in POP-based networks. These networks both prepared from the endcapped oligomer and the functional SSQO cluster, possess glass transition temperature in the range of ~ −55 to ~ −45 °C (Fig. 6). The network SD2000 shows one sharp relaxation peak at −55 °C (curve 1). The loss peak of the system EC-D2000 is smaller and broader (curve 2) and the network SPPG2000 formed under TSA catalysis exhibits two relaxation peaks at −49 and −15 °C (curve 3). The presence of TEOS in the system leads in addition to an increase in modulus also to broadening of the relaxation band and an increase in T_g (curves 4 and 5).

Interphase interaction in the O–I networks is affected to a high extent by internal structure of the SSQO domains. The high content of SiOH at the chain ends in SPPG2000 polymerized under acid catalysis results in an interaction with the oxygen of the neighboring part of the POP chain, as found by SAXS analysis. Also, loose SSQO structures formed in this case can more strongly interact with the organic matrix than the compact structures. The interaction leads to immobilization of the part of the chain close to the SSQO domain, while the middle of the chain remains free of restrictions [4,18]. Hence, two relaxation peaks in the network from SPPG2000/TSA correspond to free and constrained POP chains. The relative height of the peaks characterizes the fraction of the corresponding chains [15]. A small peak at −10 °C, in addition to the main transition peak, was also observed by Jordens and Wilkes [4] in the case of SD2000 and assigned to partially constrained chain segments at the interface between the POP and inorganic phases. Similar effects have been described in poly(tetramethylene oxide)-based O–I systems [1]. Study of the SPPG2000 networks with controlled SiOH content as shown in Fig. 7 supports the above explanation. Less silanols in the network formed using basic catalyst BDMA leads to a decrease in the interphase interaction and only one sharp relaxation peak of the free chains appears (curve 1). Also an understoichiometric amount of water ($r_{HS} < 1.5$) used for hydrolysis results in a lower content of SiOH. Only a very slight, if any, interaction was observed in the case of $r_{HS} = 0.5$ (curve 2) contrary to the conditions with the large water content, $r_{HS} = 3$ (curve 3). Moreover, no interphase interaction was found in network SD2000 undergoing an inherent base-urea catalysis in the crosslinking hydrolytic polycondensation that leads to a small silanol content. One narrow peak of the loss factor tan δ in Fig. 6 at $T_g = -55$ °C indicates relaxation of the unconfined chains only. This is consistent with SAXS results revealing a distinct microphase separation in this system. Also the SPB2000 network exhibits a sharp loss peak in Fig. 5 revealing the absence of an interaction between SSQO domains and the PB chain. In agreement with SAXS results no effect of the sol–gel catalysis in crosslinking of SPB precursors was observed.

In the EC-D2000 system, the H-bond interaction of SiOH in the cluster with the POP chain is formed when mixing both components. Thus, the random interaction occurs along all the chain and only then the system undergoes the reaction of epoxy groups in the EC with amine groups at the end of the POP chain. As a result, the whole chain could be partially immobilized and not only the chain ends close to the covalent bond to the SSQO cluster as in the case of the networks from the endcapped oligomers. The interphase interaction is reflected in a broadening of the tan δ relaxation peak in Fig. 6 (curve 2), due to distribution of the confined chain length and also in a slight shift to a higher temperature in the networks from the EC prepared under TSA or DBTDL catalysis.

The O–I networks containing TEOS show a very broad maximum of the loss factor in Fig. 6 (curves 4 and 5) corresponding to a broad distribution of immobilized chains. The strength of the interaction and fraction of confined chains increase with the TEOS content. The network chain immobilization by in situ formed silica was reported previously [4,15,19].

The ultimate mechanical properties of the O–I networks in the absence of TEOS are quite poor reaching the values; $\sigma_b = 0.5 - 1$ MPa, $\varepsilon_b = 0.2 - 0.3$, where σ_b and ε_b are, respectively, stress and elongation at break. This paper, however, was primarily intended to study the structure of the simple O–I networks with a low inorganic phase content. Nevertheless, the results reveal that O–I networks from functional SSQO clusters show better mechanical properties compared to those from endcapped oligomers. They exhibit a higher modulus and higher tensile strength at the same or even higher elongation at break, corresponding to higher toughness of the material. The optimum mechanical properties of the O–I networks with high silica contents will be investigated in a future paper. The knowledge of network structure formation from the present work will be used to optimize synthesis of thin network films used as coating materials with improved ultimate properties.

4. Conclusions

The O–I networks prepared from O–I precursors show structure, morphology and properties dependent on the type of the precursor and crosslinking mechanism. The two types of the O–I precursor used—ASO and epoxy-functional SSQO clusters (EC)—were crosslinked by hydrolytic condensation of the alkoxysilanes and by reaction of epoxy groups with diamines, respectively. In both cases the network junctions are formed by SSQO domains interconnected with organic chains. The hybrid thus is the O–I block copolymer network.

The hybrids are microphase-separated with a regular arrangement of the SSQO structures in the organic matrix. The networks from ASO exhibit a greater degree of ordering and contain small SSQO junctions in the range of 1–3 nm, whose structure depends on catalysis of the crosslinking sol–gel process. Whereas loose branched siloxane/SSQO structures are present in the networks crosslinked under acid catalysis, the compact polyhedral SSQO—'cages'—form the network junction in the case of basic or DBTDL catalysts. The networks from EC and the diamine show larger SSQO clusters the size and shape of which depend on the content of the oligomeric amine. The spherical domains 5–15 nm in diameter present the junctions in the stoichiometric networks EC-D2000. At diamine deficiency the SSQO clusters produce large cylinders of 30–150 nm in diameter. The SSQO cylinders are interconnected forming a ladder-like SSQO network with continuous SSQO structure.

Interphase H-bond interaction between SiOH in SSQO and an oligomer chain is an important factor influencing morphology. Acid catalysis of the sol–gel process, promoting hydrolysis, increases the SiOH content. Moreover, formation of loose structures leads to possibility of making strong interactions. As a result, immobilization of a part of the organic chain occurs in dependence on the O–I precursor type and polymerization procedure. While only chain ends close to attachment to the hard SSQO structures are confined in the case of ASO-based networks, SPPG2000/TSA, a broader distribution of confined sequences along the chain is present in the EC-D2000 network. The interactions strengthen in the presence of TEOS. The chain immobilization leads to a corresponding increase in glass transition temperature.

Mechanical properties and modulus of the heterogeneous O–I networks are determined by crosslinking density and morphology. EC-based networks exhibit a higher elastic modulus compared to the networks from ASO, SPPG2000 and SD2000, because of a higher crosslinking density. In addition, these networks show better ultimate mechanical properties, like strength at break and toughness. However, mechanical properties of the studied O–I networks are poor and only the presence of TEOS, increasing the fraction of an inorganic phase dispersed in the organic matrix, leads to a significant reinforcement and improvement of mechanical properties. Mainly the O–I bicontinuous morphology at a high TEOS content leads to a remarkable increase in modulus. Quite reasonable agreement of the experimental and theoretical moduli was obtained by using classic Flory–Erman theory and taking into account reinforcement with hard filler domains, according to the Kerner model or bicontinuous morphology, by using Davies approach.

Acknowledgements

The authors acknowledge financial support of the Grant Agency of Academy of Sciences of the Czech Republic (A4050008) and the Grant Agency of the Czech Republic (203/01/0735).

References

[1] Huang HH, Wilkes GL. Polym Bull 1987;18:455–62.
[2] Matějka L, Dukh O, Meissner B, Hlavatá D, Brus J, Strachota A. Macromolecules 2003;36:7977–85.
[3] Matějka L, Dukh O, Hlavatá D, Meissner B, Brus J. Macromolecules 2001;34:6904–14.
[4] Jordens K, Wilkes G. Pure Appl Chem 2000;37:145–75. 177–203.
[5] Surivet F, Lam TM, Pascault JP, Mai C. Macromolecules 1992;(25): 5742–51.
[6] Rodrigues DE, Brennan AB, Betrabet C, Wang B, Wilkes GL. Chem Mater 1992;4:1437–46.
[7] Mark JE. Polym Engng Sci 1996;36:2905–20.
[8] Matějka L, Dukh O, Brus J, Simonsick WJ, Meissner B. J Non-Cryst Solids 2000;270:34–47.
[9] Brinker CJ, Scherer GW. Sol–gel science. San Diego: Academic Press; 1990.
[10] Cuney S, Gerard JF, Dumon M, Pascault JP, Vigier G, Dušek K. J Appl Polym Sci 1997;65:2373–86.
[11] Erman B, Flory PJ. J Chem Phys 1978;68:5363–9.
[12] Dušek K, Šomvársky J. Faraday Discuss 1995;101:147–58.
[13] Nielsen LE, Landel RF. Mechanical properties of polymers and composites. New York: Marcel Dekker; 1994.
[14] Davies WEA. J Phys D: Appl Phys 1971;4:1176–81.
[15] Matějka L, Dukh O, Kolařík J. Polymer 2000;41:1449–59.
[16] Zelenka J, Ilavský M, Dobáš I, Dušek K. Polym Networks Blends 1991;1:93–101.
[17] Matějka L. Macromolecules 2000;33:3611–9.
[18] Brik M, Titman J, Bayle JP, Judenstein P. J Polym Sci, Polym Phys 1996;34:2533–42.
[19] Matějka L, Dušek K, Pleštil J, Kríž J, Lednický F. Polymer 1999;40: 171–81.